Hindawi
Advances in Materials Science and Engineering
Volume 2022, Article ID 1712207, 10 pages
https://doi.org/10.1155/2022/1712207

Research Article

Extraction of Cellulose from Sugarcane Bagasse Optimization and Characterization

Getu T. Melesse,[1] Fekadu G. Hone,[2] and Mulualem A. Mekonnen[1]

[1]*Faculty of Materials Science and Engineering, Jimma Institute of Technology, Jimma University, P. O. Box: 378, Jimma, Ethiopia*
[2]*Department of Physics, Addis Ababa University, P.O. Box: 1176, Addis Ababa, Ethiopia*

Correspondence should be addressed to Mulualem A. Mekonnen; muabeme@gmail.com

Received 1 July 2022; Revised 31 August 2022; Accepted 26 September 2022; Published 10 October 2022

Academic Editor: Jirapornchai Suksaeree

In this study, cellulose was extracted from sugarcane bagasse (SCB) through a convenient five-step treatment, and procedures were performed. During the alkaline curing process of the extraction of cellulose, NaOH has a concentration of (0.5, 1.5, 2.75, and 4%) and the extraction time (15, 30, and 45 min) at a constant temperature of 120°C were taken as variables and perfectly optimized by response surface methodology (RSM) for cellulose with the highest product. The optimum conditions were found to be 2.75% NaOH, 120°C, and 45 min with a cellulose yield of 73.71 ± 0.67% cellulose, 17.22 ± 0.82% hemicellulose, and 9.07 ± 0.95% lignin. Though most of the lignin was eliminated during the alkaline and dilute acid pretreatment process, the remaining lignin was removed by a solution treatment of 4% NaOH, and 21.92% H_2O_2 at 121°C for 44.97 min where the cellulose yield was found as 89.75 ± 0.64%, hemicellulose was 6.15 ± 0.83%, and lignin was 2.65 ± 0.66%. Morphological analysis revealed that the average diameter of the cellulose was 12.06 μm. Thermal and XRD diffraction analysis showed that the cellulose is thermally stable and has a crystallinity index of 31.63%. FTIR spectra demonstrate that cellulose was successfully extracted due to the removal of noncellulose components.

1. Introduction

The main constituent of plant biomass is lignocellulosic materials such as lignin, hemicellulose, and cellulose. Agricultural byproducts from plant biomass can serve as sustainable, renewable, and inexpensive raw materials for the production of industrial biopolymers [1]. For example, the cellulose content of SCB is around 40–50% [2]; isolated cellulosic fibers and their derivatives have attracted attention for their applications ranging from paper, packaging, sensors, water purification, and textiles to biomedical devices and drug delivery due to their advantageous properties such as low density, high surface area, and good mechanical strength [3–9]. Hemicellulose is an amorphous polymer usually composed of different types of C6 and C5 sugars: D-glucose, D-xylose, D-mannose, D-galactose, L-arabinose, D-glucuronic acid, and L-fucose. Hemicellulose is amorphous [10] and a large and complex carbohydrate molecule that helps cross-link cellulose fibers in plant cell walls [11]. Furthermore, hemicelluloses can form hydrogen bonds with cellulose and lignin, which is why they are called "cross-linking glucans" [12]. The chemical structure of hemicellulose is shown in Figure 1.

Lignin is composed of phenylpropane polymeric units, which has high resistance to chemical and physical influences and is insoluble in water. The main function of lignin is to hold fibers together. The major components of lignin are p-hydroxyphenyl, guaiacyl, and syringyl as shown in Figure 2.

Cellulose is the largest and most important natural biopolymer present in plants in the form of microfibrils and is known for its turnover capacity, biocompatibility, and biodegradability [15]. The molecular structure of cellulose consists of hydroxyl groups in the chain, which can easily form chemical bonds with various compounds to create many derivatives [16], shown in Figure 3. This leads to multiple technological uses of cellulose including transportation of drugs [17], polymer fillers [18], gases,

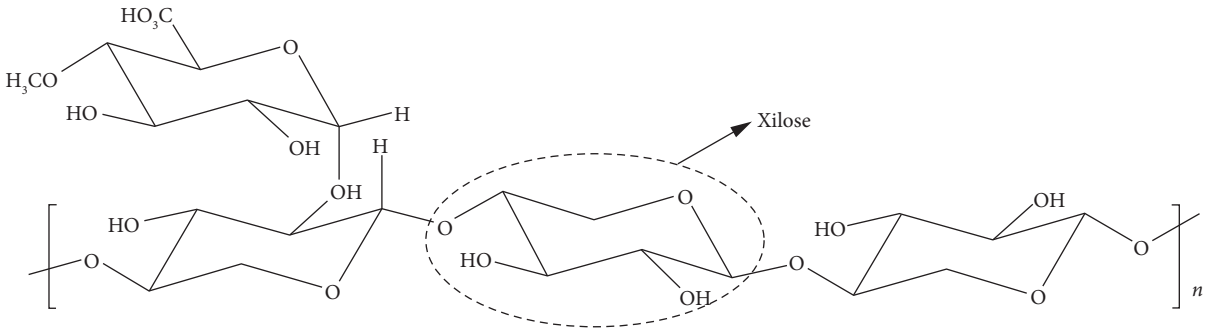

Figure 1: Chemical structure of hemicellulose [13].

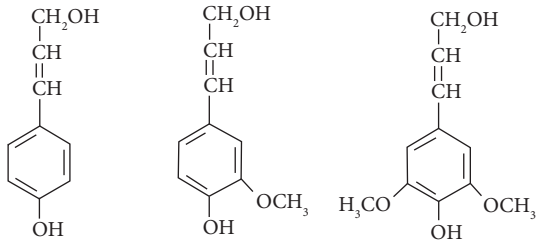

Figure 2: Structure of the main subunits of lignin precursors [14].

consumables, meals, papermaking, fabrics, and many more. This provides a compelling starting material for a wide range of industrial applications and has generated considerable research interest. Cellulose is a polymer consisting of anhydro glucose fractions bonded to carbon atoms four and one through b-glycosidic bonds. This is corroborated by the existence of 3 hydroxyl groups with reactivity, OH secondary to C-2, OH secondary to C-3, and OH number one to C-6, and therefore by the establishment of numerous van der Waals, and hydrogen bonds within solid molecule [19]. It is organized into fibrils surrounded by a matrix of lignin and hemicellulose. Currently, it seems to be common knowledge that cellulose I has a parallel chain orientation, while in cellulose II, the chains are antiparallel [20].

There is no doubt that the natural resources available to the world population are limited. Society is currently facing a number of ecological and social challenges such as global population growth, climate change, and the destruction of ecosystems, which require the definition of new production and consumption patterns that are economically, socially, and ecologically sustainable. In this context, the bioeconomy can provide a clear answer, contributing to the equitable supply and distribution of food, to mitigate the effects of climate change and to reduce the use of fossil fuels. Furthermore, it can offer new opportunities for economic development and employment. The biorefinery strategy has been identified as a key element in fostering the arising bioeconomy by providing a broad variety of products from a large collection of biomass sources to meet diverse society demands [21]. Biorefineries are a crucial instrument for the development of the bioeconomy, with the aim of providing a wide range of product collections from a broad span of biomass sources to reach the diverse needs of the community [22]. In the broadest sense, a biorefinery can be defined as a facility that produces a large area of different products through the use of different biomass feedstocks.

Numerous pretreatment methods for biomass delignification have been reported, including physical, biological, chemical, and combined methods (ammonia fiber blast and vapor) [23–29]. In fact, each pretreatment process has its pros and cons; For example, physical pretreatment such as grinding and milling requires fewer chemicals but consumes a lot of energy, especially in large-scale production [19], while the biological treatment process reduce lignin and hemicellulose, but the hydrolysis process needs overlong time [29–31]. The chemical pretreatment process is a well-studied pretreatment technique which produces a myriad of harmful chemicals, such as hydrogen sulfide [32]. The dilute acid pretreatment method can get rid of hemicellulose, but corrodes instruments and harms the environment [33]. Alkaline pretreatment process is to a greater extent appropriate for enzymatic hydrolysis as it effectively removes lignin and limits carbohydrate degradation compared to other similar methods [34]. This method incorporates sodium hydroxide, lime, ammonia, and alkaline hydrogen peroxide (AHP) chemicals for pretreatment process [34, 35]. Among the alkali-based pretreatments, hydrogen peroxide (H_2O_2) is widely utilized in the pulp firm to whiten and enhance the transparency of the paper. The usage of H_2O_2 causes the production of hydroperoxyl anion at an alkaline pH (pH 11.5), which is the main cause of the dissolution of lignin and hemicellulose [36]. Many researchers help in the development of AHP pretreatment to enhance the enzymatic hydrolysis of lignocellulosic raw materials [37–39]. For example, Su et al. fractionated hemicellulose and lignin from corn cobs with a pull out ratio of 38.7% and 75.4%, respectively, after 6 h of treatment with AHP [39].

We report a simple five-step process which is an efficient and environmentally advantageous method for extracting cellulose from SCB. In addition, the properties of the extracted cellulose were characterized and analyzed. The extracted cellulose has a good index of crystallinity, very good thermal stability, and high cellulose content under alkaline AHP bleaching conditions. This study reports the utility of sugarcane bagasse and its cellulose as reinforcing fillers for polymers composites.

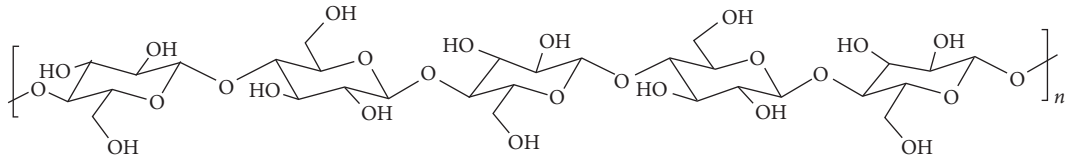

Figure 3: Chemical structure of cellulose molecule [14].

2. Experiment

2.1. Materials. The SCB sample was taken and left air dried for 24 hours. The dried SCB was kept in an oven at 100°C for 8 h to bring the moisture content to 8–10%. The dried SCB was physically fractionated with 4 mm and 3 mm mesh particle sizes and stored in an airtight polyethylene plastic bag to keep the sample dry for further research phase. The macromolecular composition of fractionated dried SCB is referred in Table 1. The chemicals used are purchased from the local representatives of Merck and Sigma-Aldrich, Ethiopia, the chemicals are sodium hydroxide (NaOH) (AR, Assay 98%), sodium hypochlorite (NaOCl), acetic acid, sulfuric acid (H_2SO_4) (AR, 98% Assay), hydrogen peroxide (H_2O_2) (the 30% ACS reagent contains inhibitors), ethanol (AR, C_2H_5OH) (>99%).

2.2. Optimization and Extraction of Cellulose

2.2.1. Pretreatment Stages: Dewaxing, Boiling, and Washing. The physically fractionated SCB, first dewaxed for about 4 h using an ethanol/DI water mixture (1:1 v/v), and the mixture is boiled for 1.5 h, this process is repeated twice to wash and dirt, dust, Earth, marrow, sugar extracts and those water-soluble impurities.

The dewaxed SCB powder was washed thoroughly with DI water at a temperature of 95°C, followed by cold DI water to remove some of the residual sugar and surfactants. It was air dried for 24 h and then dried in an oven (model 30–1060, GmbH, Germany) to constant weight at 85°C for 16 h. The humidity of the sample is maintained at about 10% (on a dry basis) with a moisture analyzer (SARTOTIUS AG GERMANY, MA 35 M-000230V2) for subsequent chemical treatments and characterization applications. The chemical composition of dewaxed SCB is given in Table 1.

2.2.2. Optimization of Alkali Treatment Conditions. NaOH-alkali treatments were carried out on the dried, crushed, ground, and sieved sample obtained after the completion of the pretreatment steps and after the determination of the experimental tests using a statistical general factorial design (GFD) methodology. The experimental design had two factors: concentrations of NaOH (A) (0.5, 1.5, 2.75 and 4%) and reaction times (B) (15, 30 and 45 min.) at a constant temperature of 120°C, for a total of $4 * 3 = 12$ treatment combinations. The quadratic model (QM) was used and comprised of 24 experimental runs, incorporating double replication for each of the treatments. Computational analysis data were collected gravimetrically based on the method developed by Chesson (2016) and the results are compiled in Table S1 in Supporting Information (SI).

2.2.3. Optimization for Dilute Acid Treatment Conditions. The experimental trials were determined using GFD statistical methodology. The experimental design had two factors: concentrations of dilute sulfuric acid (A) (0.5, 2.5, and 5%) and reaction times (B) (15 and 30 min.) with a total of $3 * 2 = 6$ main treatment combinations and a QM consisting of 12 serial experiments used, including duplicate replicates for each of the treatment conditions. The treatment of the same solid charge (5%) of sugarcane bagasse was carried out in a water bath (Sr.N. 106544116, Germany) under reflux at a constant temperature of 100°C while the amount of solid became liquid (H_2SO_4), the ratio was kept constant at 1:10 (g/ml). The contents are separated from the solid fraction by vacuum filtration. The remaining solids were washed thoroughly with warm DI water to neutral pH and oven-dried at 105°C overnight. The sample moisture was maintained at approximately 8–10% (dry basis). Then, the data on the composition analysis of the amount of SCB treated with dilute sulfuric acid of extracted cellulose, hemicellulose, and lignin were collected by gravimetry based on the method developed by Chesson [40], and the results are summarized in Table S2 in SI. The percentage of each of the collected data was calculated using a general factorial design from Design-Expert software (Stat-Ease Inc., version 7.0) for statistical analysis to determine an optimal treatment combination. Furthermore, a regression model was developed between the optimal response (as a dependent variable) and the optimal treatment combination (as independent variables).

2.2.4. Optimization for First-Step Bleaching Treatment Conditions. In addition to the alkaline pretreatment, the insoluble residue was refined and washed with distilled water. Although most of the lignin was eliminated during the alkaline pretreatment process, the remaining lignin was extracted using 1% NaOCl solution at 95°C for 60 minutes. This step was repeated twice, then, the cellulose was sieved and rinsed with distilled water until the pH of the filtrate became neutral. Finally, the resulting cellulose was dried in a hot air oven at 50°C for 24 hours. The RSM methodology was used using Design-Expert software to optimize effective parameters in the first stage bleaching process, which recovers cellulose and hemicellulose and lignin concentrations are minimized, shown in Table 2. Three factors and a QM consisting of 20 combinations of experimental procedure were used for the first-stage bleaching pretreatment process,

Table 1: Chemical composition of untreated and dewaxed sugarcane bagasse determined by the Chesson method of gravimetric analysis.

SN	Sample	Sample kind	Moisture (%)	Cellulose (%)	Hemicellulose (%)	Lignin (%)	Ash (%)	Extractives (%)	Total
1	A	Untreated	6	42.40	25.20	19.70	3.01	9.69	100
2	B	Dewaxed	6	58.86	18.79	17.60	2.25	2.50	100

Table 2: Description of the first four optimized predicted solutions of the RSM quadratic model Design matrix for the first-step bleaching treatment.

Model parameter			Yields				
Factors used in ANOVA			Y1, cellulose (%)	Y2, hemicellulose (%)	Y3, lignin (%)	Desirability	Rank
1A: Acidified NaOCl (%)	2B: Time (min)	3C: Temp (°C)	Pred.	Pred.	Pred.		
1	5	75.00	86.86 ± 0.35	7.90 ± 0.48	5.01 ± 0.25	0.969	1st
1	5	75.12	86.79 ± 0.74	7.89 ± 0.64	5.017 ± 0.93	0.966	2nd
1	5	75.00	86.80 ± 0.81	7.88 ± 0.86	5.022 ± 0.69	0.966	3rd
1	4.98	75.00	86.75 ± 0.77	7.89 ± 0.90	5.019 ± 0.75	0.962	4th

of which 6 replicates were performed. The design variables considered the lower and higher levels of 5 individual runs in each of the three factors, such as concentration of NaOCl acidified to pH 3–5 (adjusted with 1 M glacial acetic acid) (1A) (0, 1, 1.5, 2, and 2.34% by %), extraction temperatures (2B) (68, 12, 75, 85, 95, and 101.82 in °C) and extraction time (3C) (2.99, 3.5, 4.25, and 5.51 in hours), while the ratio of solids (sugarcane bagasse) to liquid (acidified NaOCl) was kept constant at 1:10 (g/ml).

The first stage of bleach solution processing was accomplished in a vertical autoclave furnished with digital temperature and time controls while reaction variables such as cellulose yield, hemicellulose, and lignin of sugarcane bagasse were evaluated. The samples with the highest cellulose concentrations and with the lowest lignin and hemicellulose concentrations were selected from the dilute sulfuric acid pretreatment process. After boiling, the liquid contents were separated from the solid parts through vacuum filtration. The remaining solids were washed thoroughly with warm deionized water to neutral pH and oven-dried at 105°C for 15 h. Sample humidity maintained at approximately 8–10% (dry basis) for later chemical treatments and characterizations and kept in sealed polythene bags at room temperature. Subsequently, the compositional analysis data from the first bleaching process for the extracted cellulose, hemicellulose, and lignin were collected gravimetrically according to the method [40].

2.2.5. Optimization for Second-Step Alkaline Hydrogen Peroxide (AHP) Bleaching Treatment Conditions. The bleaching process was completed by evaluating the effect of second stage alkaline hydrogen peroxide (AHP) solutions at pH 11–12.5 under the conditions of the bleaching process. It was performed to remove hemicellulose and lignin from SCB with a small modification of the method described by Sun et al. [26]. The RSM design was used to optimize the best combination of second stage bleaching process parameters for cellulose extraction as reported in Table 3. The study used five factors as a parameter used in the QM consisting of 50 combinations of experimental treatments were employed for investigation. The design parameters were the high and low levels of 5 individual runs in each of the five factors of NaOH concentration, H_2O_2 concentration, temperature required for extraction, extraction time, and extraction pressure, while the response variables were the yield of cellulose, hemicellulose, and lignin. The second bleaching solution treatment was carried out in a vertical autoclave (VSL series, equipped with digital temperature, pressure, and time control) while maintaining the solid to liquid ratio (mixtures of NaOH–H_2O_2) constant at 1:10 (g/ml). After boiling, the insoluble residue was collected under vacuum filtration and washed heavily with deionized water at neutral pH to take away all soluble materials. The left over white paste residue was oven-dried at a temperature of 105°C for 24 h and referred to as "purified cellulose." The humidity of sample was sustained around 8–10% (dry basis) for the next chemical treatments and characterizations and stockpiled in fasten polythene bags at room temperature. Subsequently, the data for the compositional analysis of the amount of cellulose, hemicellulose, and lignin extracted from the sugarcane bagasse treated in the second bleaching step were collected gravimetrically according to the method developed by Chesson. Percentages of all data collected from the gravimetric analysis were calculated in STATISTICA Design-Expert software and used for statistical and graphical analysis to determine the optimal treatment mix.

The X-ray diffraction of the powder was carried out using Drawell XRD 7000 with the Johanson monochromator in the incident beam to remove the Cu-Kα2 radiation. The crystallinity index (CI) was calculated using equation (1), [41].

$$CI\,(\%) = \left[\frac{(I_{002} - I_{\text{am}})}{I_{002}}\right] \times 100, \quad (1)$$

where I_{002} is the maximum intensity of the (002) diffraction at 2θ value of about 22.2°, while I_{am} is the intensity diffraction at 2θ value of around 18°.

Table 3: Description of the first three optimized predicted solutions of the RSM quadratic model design matrix for the second-step bleaching treatment.

Model parameter					Yields				
Factors used in ANOVA					Y1, cellulose (%)	Y2, Hemicellulose (%)	Y3, lignin (%)	Desirability	Rank for the selection
1A: Conc. Of NaOH (%)	2B: Conc. Of H_2O_2 (%)	3C: Time (min)	4D: Temp (°C)	5E: Pressure (Psi)	Pred.	Pred.	Pred.		
4.00	21.92	44.97	121.0	15.0	89.75 ± 0.64	6.14 ± 0.83	2.65 ± 0.66	0.97	1st
4.00	20.94	45.00	120.9	15.0	89.70 ± 0.58	6.17 ± 0.73	2.69 ± 0.96	0.97	2nd
3.89	20.52	45.00	120.9	15.0	89.75 ± 0.67	6.20 ± 0.40	2.73 ± 0.87	0.97	3rd

3. Results and Discussion

3.1. Cellulose Extraction. The chemical compositions of SCB at the beginning are 42.40% of cellulose, 25.20% of hemicellulose, and 19.70% of lignin, 3.01% of ash and 9.69% of extractives as raw materials in this study. This result is in good harmony with the work of Bruna et al. reported that 42.20% of cellulose, 27.60% of hemicellulose, 21.60% of lignin, 2.84% of ash, and 5.83% of extractives [42]. The chemical composition of the SCB after dewaxed with a 1:1 ratio of ethanol to water mixture, boiled, washed, and dried was 58.86% of cellulose, 18.79% of hemicellulose, 17.60% of lignin, and 2.25% of ash. The yields of the cellulose extracted from the SCB after treatment with NaOH-alkali were 73.57%, hemicellulose 17.225%, and lignin 9.075%. The content of cellulose in the sample through the dilute acid pretreatment stage was 82.73% and the hemicellulose and lignin components were obtained with a minimum amount of 9.21% and 7.955%, respectively, where concentration of diluted sulfuric acid was 0.50%, extraction temperature was 100°C, and extraction time was 15 minutes. After first-step bleaching treatment, we obtained the cellulose extracted from the sugarcane bagasse with a maximum expected yield of 86.86% and the hemicellulose and lignin components were obtained in a minimum amount of 7.89% and 5.01%, respectively, using with an acidified NaOCl concentration of 1.00% by weight, a reaction time of 5:00 hours, and a reaction temperature of 75°C. The result of cellulose content in the sample through the second step bleaching treatment were 89.76%, and hemicellulose and lignin components were extracted at the lowest levels of 6.15% and 2.66%, respectively.

3.2. X-ray Diffraction (XRD). In all the samples, the diffraction peaks are observed around $2\theta = 15.3$ and 22.7°. These peaks are characteristic peaks of cellulose I, designated by the (100) and (002) planes [43], as clearly observed in Figure 4.

Table 4 shows the crystallinity index of cellulose. The CI for the untreated (A) SCB is 23.68%, while the CI for the treated cellulose materials shown increment with a value of 24.82%, 26.03%, 26.34%, 29.23%, and 31.63% in the treatment of dewaxing (B), alkali, dilute H_2SO_4 (C), first-step bleaching (E1), and second-step bleaching (E2), respectively. This is due to the increment of cellulose contain in the treated materials with values of 42.4%, 58.86%, 73.71%, 83.03%, 86.86%, and 89.76% when the sample is untreated, dewaxed, alkali-treated, dilute H_2SO_4-treated, first bleaching treatment, and second bleaching treatment, respectively.

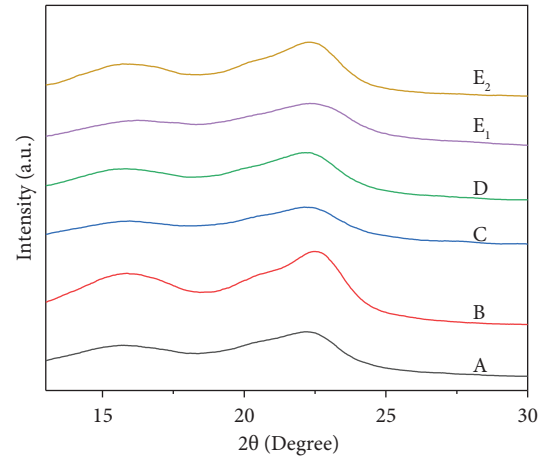

Figure 4: XRD pattern of extracted cellulose for (A) untreated, (B) dewaxing, (C) alkali, (D) dilute acidic, (E1) first bleaching, and (E2) second bleaching-treated sugarcane bagasse.

Table 4: Crystallinity index of the samples.

Sample	Crystallinity index (%)
A	23.68
B	24.82
C	26.03
D	26.34
E1	29.23
E2	31.63

The result shows CI and cellulose content has direct relationship, which was in a very good agreement with the work of Morais et al. reported a perfect linear relationship between the CI and cellulose content [44].

It has been reported that crystallinity is one of the most powerful factors in the efficiency of enzymatic hydrolysis for the reason that giant crystallinity of cellulose makes the biomass unreachable to enzymatic attack [45, 46]. The crystallinity of cellulose derived from inter- and intramolecular hydrogen bonding between cellulose chains and can be modified using biomass pretreatment technologies [47, 48]. Determining the cellulosic crystallinity of modified solids is not simple; however, because lignocellulosic

biomass consists of disordered cellulose and various noncrystalline compounds such as hemicellulose and lignin [49].

From the findings, it was concluded that the fractionation based on the five-step process modifies the chemical bonding, the structure, and the crystallinity of the cellulosic materials, but exclusively by the significant elimination of lignin since delignification contributes to increasing the crystallinity of the reclaimed materials.

3.3. Scanning Electron Microscope Analysis. The SEM image of cellulose extracted from untreated (A) sample and extracted through dewaxing stage (B), alkaline stage (C), dilute acidic stage (D), first bleaching stage (E1), and second bleaching stage (E12) process are shown in Figure 5.

There are significant changes in the morphological structure of cellulose that occurred in treated SCB samples compared to untreated SCB samples due to the removal or lesser amount of noncellulose components such as pectin, lignin, and hemicellulose.

Figure 5(a) shows the surface morphology of untreated SCB with an average cellulosic diameter of 35.23 μm surrounded with residual materials and firmly bound together in a stack, which could be because of the existence of the wax layer and intact lignocellulosic parts [43, 44]. SEM images of the deparaffinized cellulose shown in Figure 5(b) have an average cellulose diameter of 28.41 μm after removal of waxes as well as dirt, dust, soil, pith, sugar extracts, and such water-soluble impurities. There are significant differences between cellulose treated through alkaline, shown in Figure 5(c) compared to cellulose that was treated through acid hydrolysis as shown in Figure 5(d)). Based on Figure 5(c), the distribution of celluloses appeared uniform with an average diameter of 24.35 μm, while the alkaline-treated samples followed by acid hydrolysis produced cellulose with an average cellulose diameter of 17.44 μm and quite a large number of long rod-like structures, as shown in Figure 5(d). From Figure 5 (E2), the produced cellulose fibers are evenly distributed and their average width is about 12.06 μm. Therefore, the surface morphology produces the higher quality cellulose exhibited by cellulosic products have to fulfill the following treatment stages: dewaxing, alkaline, dilute acid, first stage, and second stage bleaching processes.

Figure 6 demonstrates the reduction of average diameter of cellulose, conforming the removal of waxes, lignin, and hemicelluloses, as the sample treatment continuous to different chemicals and methods, the noncellulosic components are gradually decreased to process defibrillation, resulting in a reduction in diameter.

3.4. Fourier-Transform Infrared (FTIR) Spectroscopy. Figure 7(a) and 7(b) shows the FTIR spectra of the cellulose extracted from sugarcane bagasse. All spectra showed a band in the range 3530–3050 cm^{-1}, which is ascribed to the free OH stretching vibration of the –OH group of the intermolecular and intramolecular hydrogen bonds in the cellulose molecules [45]. The spectra in Figure 7(b) manifested an absorption band around 902 cm^{-1} due to glycosidic C-H stretching vibration in cellulose molecules, representing β-glycosidic bonds and the noncrystalline portion of the cellulose [46]. The FTIR spectrum of lignin and hemicellulose indicated by peaks in the wave number around 1515 and 1732 cm^{-1} have been related to the C=C aromatic skeletal vibration of the aromatic ring in lignin and the C=O stretching vibration of hemicellulose and lignin in the structure, respectively [47, 48]. However, the various peaks associated with hemicellulose and lignin in addition to the C-H curvature of the hemicellulose and lignin structures and to the C=C vibration of the aromatic ring of lignin around 1437 cm^{-1} [49] as well as the peak at 1249 cm^{-1} attributed to out-of-plane C-O-C stretches of aryl alkyl ethers in lignin [50] decreased and almost completely disappeared in some spectra after treatment of cellulose fibers (Figure 7(b)). This was due to the reduction of hemicellulose and lignin after alkaline, dilute acid, and bleaching

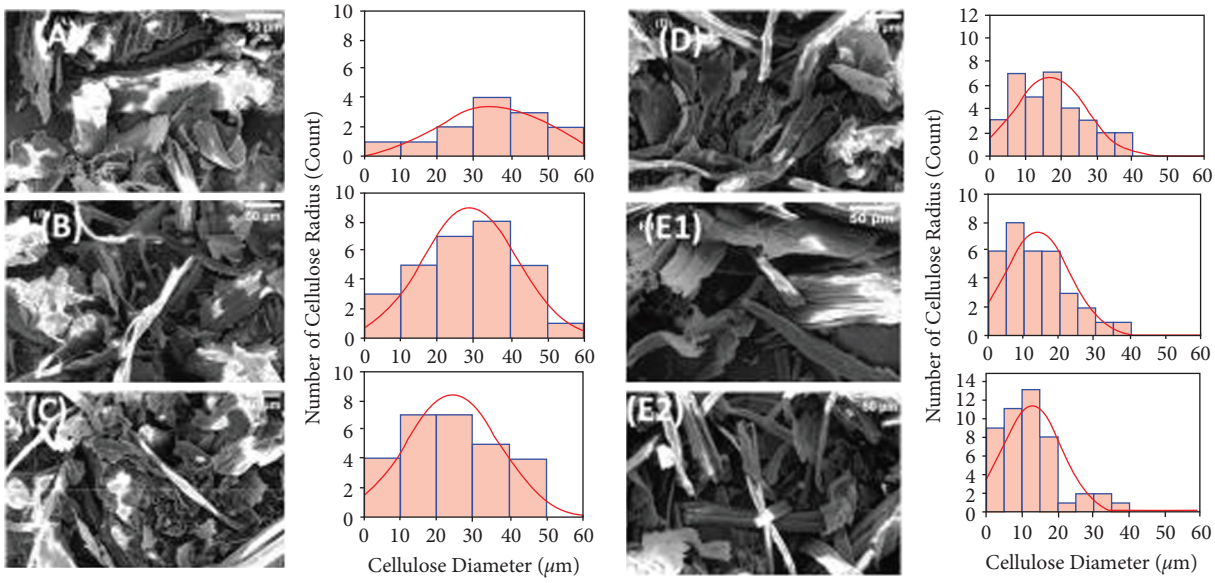

Figure 5: SEM micrographs of cellulose extracted from sugarcane bagasse.

treatments [51]. These spectra were not observed in the E2 cellulosic fibers with the exception of the peak around 902 cm^{-1} which characterizes the cellulosic structure. The outcome of the spectra illustrates the chemical treatment getting rid of most of the lignin and hemicellulose.

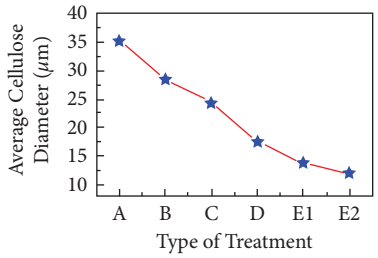

Figure 6: Average diameter of cellulose extracted from sugarcane bagasse.

3.5. Thermal Analysis. The thermogravimetric analysis (TGA) and differential thermal analysis (DTA) curves of the cellulose extracted by the different techniques are shown in Figure 8. The thermogram showed the different stages (represented by a circle in Figure 8) of degradation that takes place in the cellulose due to the differences in degradation temperature of each component of the cellulose. As shown in Figure 8(a), the initial decomposition happened at temperature between 60 and 150°C due to the evaporation of water molecules and low molecular weight components that were broken down [52].

The studied cellulosic fibers became thermally stable in the range of 220–310°C, which is associated with the onset of thermal degradation of cellulosic materials [53]. As shown in Figure 8(a), the TGA curve of all samples A, B, C, D, E1, and E2 started to decay at 232, 264, 268, 302, 310, and 312°C, respectively. The decomposition temperature at 0% weight loss for the examined samples was 347, 347.2, 360.7, 382.4,

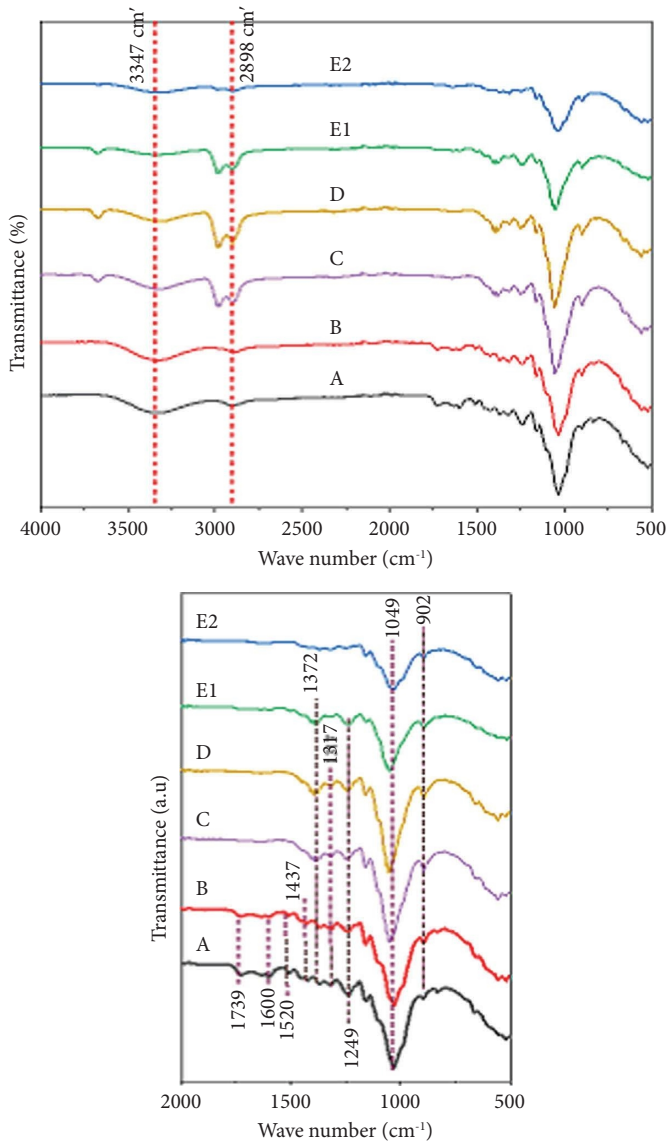

Figure 7: (a, b) FTIR spectra of the extraction of cellulose from sugarcane bagasse.

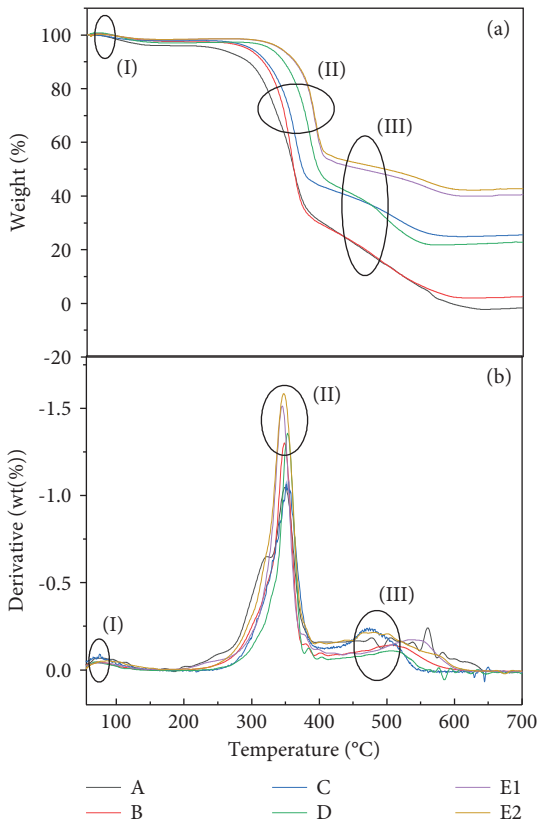

Figure 8: (a) The thermogravimetric analysis and (b) the differential thermal analysis curves of cellulose extracted from the different methods.

443.5, and 494.7°C, respectively. This was consistent with the fact that as the purity of cellulose increased, its thermal stability also increased. It is the result of the pyrolytic decomposition of the cellulose acetate polymer chain followed by deacetylation as well as the removal of the less stable lignin and hemicellulose polymer from the SCB during treatment processes [54]. The thermograph showed the different stages of temperature degradation of each component of the cellulose, which are marked with a circle in the figure. The temperature at which a 50% weight loss occurred for E1 and E2 cellulose was evident in the third stage or phase of degradation. Table 5 shows the onset of thermal decay (T_{on}) and the maximum thermal decay (T_{max}) of all samples taken from the DTA curve (Figure 8(b)).

The decomposition temperature of Sample-B with T_{max}=348°C is higher than that of Sample-A with 345°C by 3°C, but Sample-A showed higher weight losses than Sample-B as tabulated in Table 5. This is due to the reduction of the content of hemicellulose and lignin after the dewaxing pretreatment process. The T_{on} of dewaxed cellulose increased from 310 to 318°C, while cellulose-B increased slightly from 318 to 320, 321, 324, and 328°C for cellulose-C, cellulose-D, cellulose-E1, and cellulose-E2. In general, all samples show an increase in trend T_{max}, while they show a decrease in weight loss. This corresponds to the fact that thermal stability of cellulose is directly proportional to its purity. This work's thermal stability is better than the

Table 5: The onset thermal decomposition (T_{on}) and the maximum thermal decomposition (T_{max}) of all samples as collected from the DTA curve.

sample	T_{on} (°C)	Weight loss (%)	T_{max} (°C)	Weight loss (%)
A	310	24.56	345	48.33
B	318	15.04	348	47.51
C	320	13.25	352	34.04
D	321	6.10	353	19.79
E1	324	4.31	344	7.30
E2	328	3.42	352	10.00

thermal stability reported in related studies such as Arzu et al. [55]. The main thermal decomposition took place at 350–600°C. A similar result has also been obtained by other researchers where cellulose acetate undergoes a strong degradation between 330°C and 450°C [55].

4. Conclusion

Cellulose was efficiently extracted from sugarcane bagasse through a five-step process. This study showed that a large amount of hemicellulose and lignin was removed with optimal solutions of alkaline hydrogen peroxide (AHP) at pH 11–12.5 under the conditions of the bleaching process that allow for maximum cellulose yield, which has been confirmed by FTIR spectra. As a result of SEM analysis, the average diameter of cellulose was 12.06 μm. TGA and XRD analysis showed that cellulose is thermally stable and has the highest crystallinity index of 31.63%. Therefore, the applied procedures are successful for getting to the appropriate properties of cellulose. The cellulose will be highly recommended for use as fillers for polymeric composites.

Data Availability

The data used to support the findings of this study are included within the article.

Conflicts of Interest

The authors declare that they have no conflicts of interest.

Acknowledgments

The authors would like to acknowledge the support provided by the Faculty of Materials Science and Engineering at the Jimma Institute of Technology.

Supplementary Materials

Supporting Information (SI) contains the experimental section and additional information regarding the three optimized predicted solutions of the General Factorial quadratic model design matrix for NaOH-alkali treatment and dilute sulfuric acid treatment conditions with experimental values of response variables. (*Supplementary Materials*)

References

[1] A. Biswas, B. C. Saha, J. W. Lawton, R. L. Shogren, and J. L. Willett, "Process for obtaining cellulose acetate from agricultural by-products," *Carbohydrate Polymers*, vol. 64, no. 1, pp. 134–137, 2006.

[2] J. X. Sun, X. F. Sun, H. Zhao, and R. C. Sun, "Isolation and characterization of cellulose from sugarcane bagasse," *Polymer Degradation and Stability*, vol. 84, no. 2, pp. 331–339, 2004.

[3] A. Khan, Y. Wen, T. Huq, and Y. Ni, "Cellulosic nanomaterials in food and nutraceutical applications: a review," *Journal of Agricultural and Food Chemistry*, vol. 66, no. 1, pp. 8–19, 2018.

[4] J.-W. Rhim, H.-M. Park, and C.-S. Ha, "Bio-nanocomposites for food packaging applications," *Progress in Polymer Science*, vol. 38, no. 10-11, pp. 1629–1652, 2013.

[5] S. K. Yadav, Ed., *Nanoscale Materials in Targeted Drug Delivery, Theragnosis and Tissue Regeneration*, Springer, Singapore, 2016.

[6] S. Ummartyotin and H. Manuspiya, "A critical review on cellulose: from fundamental to an approach on sensor technology," *Renewable and Sustainable Energy Reviews*, vol. 41, pp. 402–412, 2015.

[7] H. Orelma, A. Hokkanen, I. Leppänen, K. Kammiovirta, M. Kapulainen, and A. Harlin, "Optical cellulose fiber made from regenerated cellulose and cellulose acetate for water sensor applications," *Cellulose*, vol. 27, no. 3, pp. 1543–1553, 2020.

[8] A. Khan, Z. Abas, H. S. Kim, and J. Kim, "Recent progress on cellulose-based electro-active paper, its hybrid nanocomposites and applications," *Sensors*, vol. 16, no. 8, p. 1172, 2016.

[9] H. Voisin, L. Bergström, P. Liu, and A. P. Mathew, "Nanocellulose-based materials for water purification," *Nanomaterials*, vol. 7, no. 3, p. 57, 2017.

[10] J. A. R. Rodrigues, "From the mill to a biorefinery: the sugar factory as an industrial enterprise for the generation of biochemicals and biofuels," *Química Nova*, vol. 34, pp. 1242–1254, 2011.

[11] C. L. Williams, A. Dahiya, and P. Porter, *Bioenergy*, A. Dahiya, Ed., pp. 5–36, Academic Press, Cambridge, Massachusetts, MA, USA, 2015.

[12] V. Pasangulapati, K. D. Ramachandriya, A. Kumar, M. R. Wilkins, C. L. Jones, and R. L. Huhnke, "Effects of cellulose, hemicellulose and lignin on thermochemical conversion characteristics of the selected biomass," *Bioresource Technology*, vol. 114, pp. 663–669, 2012.

[13] F. A. Santos, J. H. de Queiróz, J. L. Colodette, S. A. Fernandes, V. M. Guimarães, and S. T. Rezende, "Potencial da palha de cana-de-açúcar para produção de etanol," *Química Nova*, vol. 35, pp. 1004–1010, 2012.

[14] R. Smith, *Biodegradable Polymers for Industrial Applications*, CRC Press, Florida, Fl, USA, 2005.

[15] D. Illera, J. Mesa, H. Gomez, and H. Maury, "Cellulose aerogels for thermal insulation in buildings: trends and challenges," *Coatings*, vol. 8, no. 10, p. 345, 2018.

[16] L. J. R. Nunes, T. P. Causer, and D. Ciolkosz, "Biomass for energy: a review on supply chain management models," *Renewable and Sustainable Energy Reviews*, vol. 120, Article ID 109658, 2020.

[17] H. Du, W. Liu, M. Zhang, C. Si, X. Zhang, and B. Li, "Cellulose nanocrystals and cellulose nanofibrils based hydrogels for biomedical applications," *Carbohydrate Polymers*, vol. 209, pp. 130–144, 2019.

[18] T. E. Motaung and R. D. Anandjiwala, "Effect of alkali and acid treatment on thermal degradation kinetics of sugar cane bagasse," *Industrial Crops and Products*, vol. 74, pp. 472–477, 2015.

[19] J. F. Kadla and R. D. Gilbert, "Cellulose structure:a review," *Cellulose Chemistry and Technology*, vol. 34, no. 3–4, pp. 197–216, 2000.

[20] H. Lennholm and T. Iversen, "The effects of laboratory beating on cellulose structure," *Nordic Pulp and Paper Research Journal*, vol. 10, no. 2, pp. 104–109, 1995.

[21] P. Manzanares, "The role of biorefinering research in the development of a modern bioeconomy," *Acta Innovations*, vol. 37, pp. 47–56, 2020.

[22] J. Wenger and T. Stern, "Reflection on the research on and implementation of biorefinery systems – a systematic literature review with a focus on feedstock," *Biofuels, Bioproducts and Biorefining*, vol. 13, no. 5, pp. 1347–1364, 2019.

[23] O. M. Perrone, F. M. Colombari, J. S. Rossi et al., "Ozonolysis combined with ultrasound as a pretreatment of sugarcane bagasse: effect on the enzymatic saccharification and the physical and chemical characteristics of the substrate," *Bioresource Technology*, vol. 218, pp. 69–76, 2016.

[24] R. Zuluaga, J. L. Putaux, J. Cruz, J. Vélez, I. Mondragon, and P. Gañán, "Cellulose microfibrils from banana rachis: effect of alkaline treatments on structural and morphological features," *Carbohydrate Polymers*, vol. 76, no. 1, pp. 51–59, 2009.

[25] J. H. Bang and K. S. Suslick, "Applications of ultrasound to the synthesis of nanostructured materials," *Advanced Materials*, vol. 22, no. 10, pp. 1039–1059, 2010.

[26] A. Kumar, Y. Singh Negi, V. Choudhary, and N. Kant Bhardwaj, "Characterization of cellulose nanocrystals produced by acid-hydrolysis from sugarcane bagasse as agro-waste," *Journal of Materials Physics and Chemistry*, vol. 2, no. 1, pp. 1–8, 2020.

[27] D. Kim, "Physico-chemical conversion of lignocellulose: inhibitor effects and detoxification strategies: a mini review," *Molecules*, vol. 23, no. 2, p. 309, 2018.

[28] C. Cara, E. Ruiz, J. M. Oliva, F. Sáez, and E. Castro, "Conversion of olive tree biomass into fermentable sugars by dilute acid pretreatment and enzymatic saccharification," *Bioresource Technology*, vol. 99, no. 6, pp. 1869–1876, 2008.

[29] P. Kumar, D. M. Barrett, M. J. Delwiche, and P. Stroeve, "Methods for pretreatment of lignocellulosic biomass for efficient hydrolysis and biofuel production," *Industrial & Engineering Chemistry Research*, vol. 48, no. 8, pp. 3713–3729, 2009.

[30] M. R. K. Sofla, R. J. Brown, T. Tsuzuki, and T. J. Rainey, "A comparison of cellulose nanocrystals and cellulose nanofibres extracted from bagasse using acid and ball milling methods," *Advances in Natural Sciences: Nanoscience and Nanotechnology*, vol. 7, no. 3, Article ID 035004, 2016.

[31] S. S. Hassan, G. A. Williams, and A. K. Jaiswal, "Emerging technologies for the pretreatment of lignocellulosic biomass," *Bioresource Technology*, vol. 262, pp. 310–318, 2018.

[32] A. K. Mathew, A. Abraham, K. K. Mallapureddy, and R. K. Sukumaran, *Waste Biorefinery*, T. Bhaskar, A. Pandey, S. V. Mohan, D.-J. Lee, and S. K. Khanal, Eds., pp. 267–297, Elsevier, Amsterdam, Netherlands, 2018.

[33] B. S. Santucci, J. Bras, M. N. Belgacem, A. A. S. Curvelo, and M. T. B. Pimenta, "Evaluation of the effects of chemical composition and refining treatments on the properties of

nanofibrillated cellulose films from sugarcane bagasse," *Industrial Crops and Products*, vol. 91, pp. 238–248, 2016.

[34] J. S. Kim, Y. Y. Lee, and T. H. Kim, "A review on alkaline pretreatment technology for bioconversion of lignocellulosic biomass," *Bioresource Technology*, vol. 199, pp. 42–48, 2016.

[35] A. Mittal, R. Katahira, B. S. Donohoe et al., "Alkaline peroxide delignification of corn stover," *ACS Sustainable Chemistry & Engineering*, vol. 5, no. 7, pp. 6310–6321, 2017.

[36] J. M. Gould, "Studies on the mechanism of alkaline peroxide delignification of agricultural residues," *Biotechnology and Bioengineering*, vol. 27, no. 3, pp. 225–231, 1985.

[37] G. Jiang, Z. Wu, K. Ramachangra, C. Zhao, and K. Ameer, "Changes in structural and chemical composition of insoluble dietary fibers bound phenolic complexes from grape pomace by alkaline hydrolysis treatment," *Food Science and Technology*, vol. 42, no. 4, 2021.

[38] Y. Su, R. Du, H. Guo et al., "Fractional pretreatment of lignocellulose by alkaline hydrogen peroxide: characterization of its major components," *Food and Bioproducts Processing*, vol. 94, pp. 322–330, 2015.

[39] A. Chesson, "The maceration of linen flax under anaerobic conditions," *Journal of Applied Bacteriology*, vol. 45, no. 2, pp. 219–230, 2008.

[40] L. Segal, J. J. Creely, A. E. Martin, and C. M. Conrad, "An empirical method for estimating the degree of crystallinity of native cellulose using the X-ray diffractometer," *Textile Research Journal*, vol. 29, no. 10, pp. 786–794, 1959.

[41] B. S. Boneberg, G. D. Machado, D. F. Santos et al., "Biorefinery of lignocellulosic biopolymers," *Revista Eletrônica Científica da UERGS*, vol. 2, no. 1, pp. 79–100, 2016.

[42] D. Klemm, B. Heublein, H.-P. Fink, and A. Bohn, "Cellulose: fascinating biopolymer and sustainable raw material," *Angewandte Chemie International Edition*, vol. 44, no. 22, pp. 3358–3393, 2005.

[43] A. R. C. Morais, J. V. Pinto, D. Nunes et al., "Imidazole: prospect solvent for lignocellulosic biomass fractionation and delignification," *ACS Sustainable Chemistry & Engineering*, vol. 4, no. 3, pp. 1643–1652, 2016.

[44] V. P. Puri, "Effect of crystallinity and degree of polymerization of cellulose on enzymatic saccharification," *Biotechnology and Bioengineering*, vol. 26, no. 10, pp. 1219–1222, 1984.

[45] J. S. Van Dyk and B. I. Pletschke, "A review of lignocellulose bioconversion using enzymatic hydrolysis and synergistic cooperation between enzymes—factors affecting enzymes, conversion and synergy," *Biotechnology Advances*, vol. 30, no. 6, pp. 1458–1480, 2012.

[46] J. Bian, F. Peng, X.-P. Peng et al., "Effect of [Emim]Ac pretreatment on the structure and enzymatic hydrolysis of sugarcane bagasse cellulose," *Carbohydrate Polymers*, vol. 100, pp. 211–217, 2014.

[47] G. Cheng, P. Varanasi, C. Li et al., "Transition of cellulose crystalline structure and surface morphology of biomass as a function of ionic liquid pretreatment and its relation to enzymatic hydrolysis," *Biomacromolecules*, vol. 12, no. 4, pp. 933–941, 2011.

[48] H.-M. Liu, B. Feng, and R.-C. Sun, "Enhanced bio-oil yield from liquefaction of cornstalk in sub- and supercritical ethanol by acid–chlorite pretreatment," *Industrial & Engineering Chemistry Research*, vol. 50, no. 19, Article ID 10928, 2011.

[49] A. Mandal and D. Chakrabarty, "Studies on the mechanical, thermal, morphological and barrier properties of nanocomposites based on poly(vinyl alcohol) and nanocellulose from sugarcane bagasse," *Journal of Industrial and Engineering Chemistry*, vol. 20, no. 2, pp. 462–473, 2014.

[50] L. A. S. Costa, D. J. Assis, G. V. P. Gomes, J. B. Silva, A. F. Fonsêca, and J. I. Druzian, "Extraction and characterization of nanocellulose from corn stover," *Materials Today Proceedings*, vol. 2, no. 1, pp. 287–294, 2015.

[51] W. H. Danial, Z. Abdul Majid, M. N. Mohd Muhid, S. Triwahyono, M. B. Bakar, and Z. Ramli, "The reuse of wastepaper for the extraction of cellulose nanocrystals," *Carbohydrate Polymers*, vol. 118, pp. 165–169, 2015.

[52] H. Yang, R. Yan, H. Chen, D. H. Lee, and C. Zheng, "Characteristics of hemicellulose, cellulose and lignin pyrolysis," *Fuel*, vol. 86, no. 12-13, pp. 1781–1788, 2007.

[53] N. T. Lam, R. Chollakup, W. Smitthipong, T. Nimchua, and P. Sukyai, "Characterization of cellulose nanocrystals extracted from sugarcane bagasse for potential biomedical materials," *Sugar Tech*, vol. 19, no. 5, pp. 539–552, 2017.

[54] Q. K. Beg, M. Kapoor, L. Mahajan, and G. S. Hoondal, "Microbial xylanases and their industrial applications: a review," *Applied Microbiology and Biotechnology*, vol. 56, no. 3-4, pp. 326–338, 2001.